Spacecraft Attitude Control Design with Adaptive Bounded Controllers

Sean Shan-Min Swei *

This paper presents the development of a control system design to keep the spacecraft attitude at a prescribed sun vector. A bounded controller is proposed which utilizes the measured sun vector and spacecraft spin rates, and the control gains are model independent and can be tuned for individual axis. An adaptive control scheme is developed for control parameters to ensure closed-loop performance. To demonstrate the effectiveness of proposed controller, a spacecraft engaging the sun safe-hold is simulated.

I. Introduction

An essential part of a spacecraft's attitude determination and control systems (ADCS) is a simple and reliable safe-hold mode controller that the ADCS can fall back on if the spacecraft experiences problems. The purpose of sun safe-hold is to ensure that the spacecraft is power positive; for instance by directing the solar panels toward sun, thermally safe, and instrument safe if needed. Many safe-hold modes for larger missions feature a fully redundant set of sensors, such as those implemented on Hubble[1] and the Solar Dynamics Observatory (SDO).[2] In addition, solar panels are appended via a gimbaled mechanism so that the panels can be rotated toward the sun independent of spacecraft attitude. For small spacecraft or low budget missions, complete redundancy is neither required nor affordable, and in order to save mass and for simplicity, solar panels can be rigidly attached to the spacecraft, see GRAIL.[4] Therefore, in these applications it is critical to implement reliable and robust control system designs by utilizing the basic ADCS hardware such as coarse sun sensors, rate gyros, and reaction wheels.

Since reaction wheels in practice can only deliver limited control torque, the total spacecraft control authority is bounded. However, the linear state-feedback controllers which were commonly used in most spacecraft attitude control literatures are in fact not bounded. The spacecraft attitude determination and control problem has been studied quite extensively, especially with quaternion feedback, see for example,[5,6] and the references therein. The controllers presented in these works tend to be either model dependent or utilizing scalar gains, which may not be desirable in actual implementation, since the mass and inertia properties of the spacecraft are such that each axis may demand a different control gain for specific mission requirements. Therefore, in this paper we propose a bounded nonlinear PD-type controller, in which the control gains are model independent and can be chosen for individual axis. Finally, we demonstrate the use of the results by developing an adaptive scheme for control parameters to ensure closed-loop performance.

II. Spacecraft Dynamics

The angular momentum of the rigid body spacecraft in the inertial frame is given by

$$ {}^{I}H^{sp} = J\,{}^{I}\omega^{b}\,, \tag{1} $$

where J is the mass moment of inertia of the spacecraft, excluding the reaction wheels, and ${}^{I}\omega^{b} = [\omega_x\ \omega_y\ \omega_z]^t$ is the angular velocity of spacecraft relative to the inertial frame. The total reaction wheel angular momentum relative to the inertial frame is described by

$$ {}^{I}H^{rw} = TI_{rw}T^{t}\,{}^{I}\omega^{b} + TI_{rw}\,{}^{b}\omega^{rw}\,, \tag{2} $$

where T is the conversion matrix that transforms the reaction wheel spin axis to the spacecraft body fixed frame, I_{rw} a matrix containing the reaction wheel's axial moment of inertia along its diagonal, and ${}^{b}\omega^{rw}$

*Research Scientist, Intelligent Systems Division, NASA Ames Research Center

a vector containing reation wheel's spin rate relative to the body fixed frame. Therefore, the total angular momentum for the spacecraft system is the summation of the the spacecraft angular momentum given in Eq. (1) and reaction wheel angular momentum given in Eq. (2), and is described by

$$\begin{aligned} {}^{I}H^{ss} &= {}^{I}H^{sp} + {}^{I}H^{rw} \\ &= J\,{}^{I}\omega^{b} + TI_{rw}T^{t}\,{}^{I}\omega^{b} + TI_{rw}\,{}^{b}\omega^{rw} \\ &= J_a\,{}^{I}\omega^{b} + TI_{rw}\,{}^{b}\omega^{rw} \end{aligned} \tag{3}$$

where $J_a = J + TI_{rw}T^t$. Note that in general the reaction wheel inertia is negligible compared to the spacecraft inertia, so in practice $J_a \approx J$.

Let τ_{ext} denote the total external disturbance torque, and by setting the time derivative of Eq. (3) equal to the external disturbance torque, we obtain

$$\begin{aligned} \tau_{ext} &= \frac{d^{I}\,{}^{I}H^{ss}}{dt} \\ &= \frac{d^{b}\,{}^{I}H^{ss}}{dt} + {}^{I}\omega^{b} \times {}^{I}H^{ss}\,. \end{aligned} \tag{4}$$

Substituting Eq. (3) into above yields,

$$\begin{aligned} \tau_{ext} &= (J^{I}\dot{\omega}^{b} + TI_{rw}\,{}^{b}\dot{\omega}^{rw}) + {}^{I}\omega^{b} \times (J^{I}\omega^{b} + TI_{rw}\,{}^{b}\omega^{rw}) \\ &= \underbrace{(J^{I}\dot{\omega}^{b} + {}^{I}\omega^{b} \times J^{I}\omega^{b})}_{\text{Spacecraft}} + \underbrace{(TI_{rw}\,{}^{b}\dot{\omega}^{rw} + {}^{I}\omega^{b} \times TI_{rw}\,{}^{b}\omega^{rw})}_{\text{Reaction Wheels}}\,. \end{aligned} \tag{5}$$

Let $u = [\tau_x \quad \tau_y \quad \tau_z]^t$ be the internal control torque generated by the reaction wheels, then the equal and opposite torque will be applied to the spacecraft. Therefore, Eq. (5) can be rewritten as follows,

$$J\,{}^{I}\dot{\omega}^{b} = J\,{}^{I}\omega^{b} \times {}^{I}\omega^{b} + u + \tau_{ext} \tag{6}$$

where the control torque u is defined by

$$\begin{aligned} u &= -\left(TI_{rw}\,{}^{b}\dot{\omega}^{rw} + {}^{I}\omega^{b} \times TI_{rw}\,{}^{b}\omega^{rw}\right) \\ &= -\left(T\tau_{rw} + {}^{I}\omega^{b} \times Th_{rw}\right) \end{aligned} \tag{7}$$

where τ_{rw} and h_{rw} denote respectively the reaction wheel torque and angular momentum along its spin axis. Eq. (6) represents the dynamics of the spacecraft subject to the control and disturbance inputs. This equation along with the sun vector dynamics, which will be discussed in the sequel, form a complete equation of motion for spacecraft attitude control for the sun safe mode. The control torque u can be designed by following many available references, and once it is determined, we can solve Eq. (7) for both τ_{rw} and h_{rw}, which then become the commanded input to the reaction wheels. The development of reaction wheel model is not covered in this paper.

Let $S(t)$ be the measured unit sun vector relative to the body fixed frame at time t, i.e. $\|S(t)\| = 1$. Then, the time derivative of $S(t)$ relative to the inertial frame, denoted as $\frac{{}^{I}dS}{dt}$, can be described by

$$\frac{{}^{I}dS}{dt} = \frac{{}^{b}dS}{dt} + {}^{I}\,\omega^{b} \times S\,, \tag{8}$$

where $\frac{{}^{b}dS}{dt}$ denotes the time rate change of the sun vector S relative to the body fixed frame. Since the sun vector stays almost stationary in inertial frame, we deduce that $\frac{{}^{I}dS}{dt} \approx 0$. Therefore, Eq. (8) can be simplified to

$$\frac{{}^{b}dS}{dt} = -{}^{I}\omega^{b} \times S\,, \tag{9}$$

which describes the sun vector dynamics relative to the body fixed frame. Note that the sun vector S is determined by processing the on-board sun sensor data and the spacecraft rotational rate ${}^{I}\omega^{b}$ is obtained by processing the rate gyro data. As mentioned earlier, Eqs. (6) and (9) together completely describe the spacecraft attitude dynamics, and they are given as follows,

$$\Sigma : \begin{cases} J\dot{\omega} &= J\,\omega \times \omega + u \\ \dot{S} &= -\omega \times S \end{cases} \tag{10}$$

For sake of control development, we neglect the external disturbance τ_{ext}, and use ω instead of ${}^I\omega^b$ for brevity.

III. Design of Bounded Controllers

In actual control applications, the control effort is always limited. In the case of reaction wheels, depending on how they are configured, the generated reactional control torques may differ from one axis to another, but they are limited. In this paper, we propose a bounded PD-type nonlinear controller with an inner velocity loop which is commanded from an outer sun vector loop.

Let the measured sun vector S and the target sun vector S_d be denoted as

$$S = \begin{bmatrix} S_x \\ S_y \\ S_z \end{bmatrix}, \; S_d = \begin{bmatrix} S_{dx} \\ S_{dy} \\ S_{dz} \end{bmatrix}, \tag{11}$$

and both S and S_d are unit vectors. The sun vector error S_e is calculated as the cross product of S and S_d, i.e. $S_e = S \times S_d$. If the spacecraft rotates about the error vector S_e, then the sun vector S will be driven toward the target sun vector S_d, hence the attitude error S_e will be diminished. We propose the following bounded controller,

$$u = -K_p \left(S - S_d\right) \times S - K_d \, \mathrm{Tanh}(\bar{a}\omega), \tag{12}$$

where $K_p = \mathrm{diag}(K_{px}, K_{py}, K_{pz})$ and $K_d = \mathrm{diag}(K_{dx}, K_{dy}, K_{dz})$ are positive definite matrices respectively denoting the attitude and rate control gains, and they are determined in the sequel. $\mathrm{Tanh}(\cdot)$ is a vector of Sigmoid functions defined by

$$\mathrm{Tanh}(\bar{a}\omega) = \begin{bmatrix} \tanh(a_x\omega_x) \\ \tanh(a_y\omega_y) \\ \tanh(a_z\omega_z) \end{bmatrix}, \tag{13}$$

where (a_x, a_y, a_z) are positive scalars and represent the slopes of Sigmoid functions at the origin. Furthermore, they can be tuned to improve performance, if needed. Note that $\tanh(\cdot)$ is hyperbolic function bounded by 1. Utilizing Eqs. (11) and (13), we can rewrite (12) as

$$\begin{bmatrix} u_x \\ u_y \\ u_z \end{bmatrix} = \begin{bmatrix} -K_{py}S_z(S_y - S_{dy}) + K_{pz}S_y(S_z - S_{dz}) - K_{dx}\tanh(a_x\omega_x) \\ -K_{pz}S_x(S_z - S_{dz}) + K_{px}S_z(S_x - S_{dx}) - K_{dy}\tanh(a_y\omega_y) \\ -K_{px}S_y(S_x - S_{dx}) + K_{py}S_x(S_y - S_{dy}) - K_{dz}\tanh(a_z\omega_z) \end{bmatrix}. \tag{14}$$

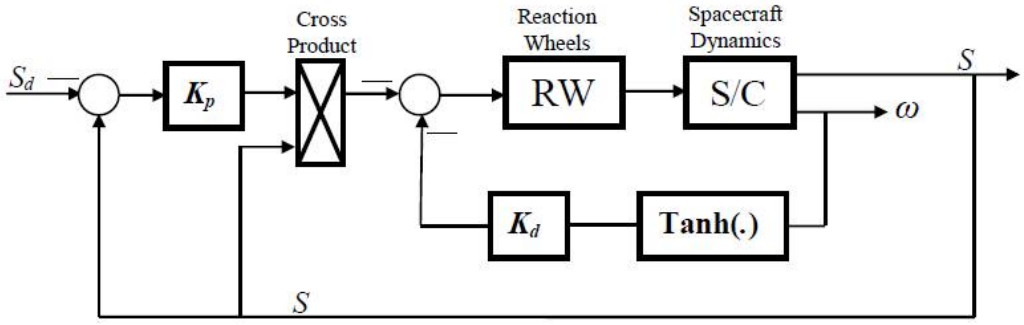

Figure 1. Block diagram for Sun Safe-Hold Control

Based on the maximum torque of each reaction wheel and the number of reaction wheels and their placement onboard the spacecraft, the control torque authority at each axis in the body fixed frame can be

pre-determined. We let $(\bar{u}_x, \bar{u}_y, \bar{u}_z)$ to denote the control torque limits. Therefore, the control u in (12) is constrained by

$$\frac{u_x^2}{\bar{u}_x^2} + \frac{u_y^2}{\bar{u}_y^2} + \frac{u_z^2}{\bar{u}_z^2} \leq 1\,, \tag{15}$$

or in compact form,

$$u^t R u \leq 1\,;\; R = \text{diag}\left(\frac{1}{\bar{u}_x^2}\,,\, \frac{1}{\bar{u}_y^2}\,,\, \frac{1}{\bar{u}_z^2}\right).$$

In other words, the control vector u is always within the ellipsoid defined by (15), see Figure 2.

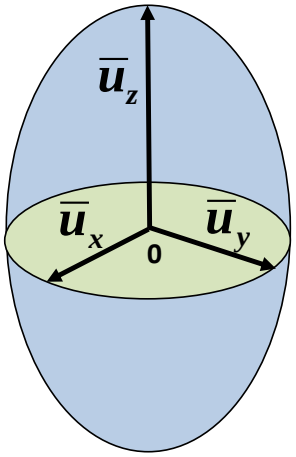

Figure 2. An ellipsoid formed by control torque limits.

By substituting (14) into above and noting that both S and S_d are unit vectors, we can derive that the control gains $K_p > 0$ and $K_d > 0$ must satisfy

$$\frac{K_y^2 + K_z^2 + K_{dx}^2}{\bar{u}_x^2} + \frac{K_x^2 + K_z^2 + K_{dy}^2}{\bar{u}_y^2} + \frac{K_x^2 + K_y^2 + K_{dz}^2}{\bar{u}_z^2} \leq 1\,. \tag{16}$$

It is left to show that the proposed bounded nonlinear controller (12) globally asymptotically stabilizes (10). To prove this, we first substitute (12) into (10) to form a closed-loop system representation described by

$$\Sigma_c\,:\, \left\{ \begin{array}{rcl} J\dot{\omega} & = & J\,\omega \times \omega - K_p\,(S - S_d) \times S - K_d\,\text{Tanh}(\bar{a}\omega) \\ \dot{S} & = & -\omega \times S \end{array} \right. \tag{17}$$

In what follows, we prove that Σ_c is globally asymptotically stable. Let

$$V(\omega, S) = \frac{1}{2}\omega^t J \omega + \frac{1}{2}(S - S_d)^t K_p (S - S_d) \tag{18}$$

be a candidate Lyapunov function for Σ_c, where $K_p > 0$ is given in (12). Note that the function $V \geq 0$ for all ω and S, and that $V = 0$ only at the equilibrium, $\omega = 0$ and $S = S_d$. If K_p is a scalar, then $V = \frac{1}{2}\omega^t J \omega + K_p\,(1 - S_d^t\,S)$, and the prove for global stability in this case is relatively straightforward.

The time derivative of $V(\omega, S)$ is given by

$$\dot{V} = \omega^t J \dot{\omega} + (S - S_d)^t K_p \dot{S}\,.$$

Now, substitute (17) into above, we obtain

$$\begin{aligned}
\dot{V}(\omega, S) &= \omega^t(J\,\omega \times \omega) - \omega^t[K_p\,(S - S_d) \times S] - \omega^t K_d \mathrm{Tanh}(\bar{a}\omega) + (S - S_d)^t K_p(-\omega \times S) \\
&= -\omega^t K_d \mathrm{Tanh}(\bar{a}\omega) - \omega^t[K_p\,(S - S_d) \times S] + (S - S_d)^t K_p(S \times \omega) \\
&= -\omega^t K_d \mathrm{Tanh}(\bar{a}\omega) - \omega^t[K_p\,(S - S_d) \times S] + \omega^t[K_p\,(S - S_d) \times S] \\
&= -\omega^t K_d \mathrm{Tanh}(\bar{a}\omega) \\
&= -\omega_x\,K_{dx}\tanh(a_x\omega_x) - \omega_y\,K_{dy}\tanh(a_y\omega_y) - \omega_z\,K_{dz}\tanh(a_z\omega_z) \\
&\leq 0
\end{aligned} \tag{19}$$

for all ω and S. In attaining the above, we have applied the vector triple product identity and the fact that K_d is a positive definite matrix and $\tanh(X) \geq 0$ if $X \geq 0$ or $\tanh(X) < 0$ if $X < 0$. To prove global asymptotic stability, we need to show that $\dot{V} = 0$ only at the equilibrium, $\omega = 0$ and $S = S_d$. From (19), we note that $\dot{V} = 0$ for all $t \geq 0$ implies $\omega = 0$ for all $t \geq 0$, hence $\dot{\omega} = 0$ for all $t \geq 0$. Thus, from the second equation of (17), we note that $\dot{S} = 0$ for all $t \geq 0$, which implies that S is a constant. Now, substituting $\dot{\omega} = 0$ and $\omega = 0$ into the first equation of (17) yields

$$K_p\,(S - S_d) \times S = 0\,, \tag{20}$$

which implies that the vector $K_p(S - S_d)$ and the measured sun vector S are in parallel. Hence, we can deduce that

$$K_p(S - S_d) = c\,S\,, \tag{21}$$

where c is some constant. Since K_p is invertible, we can rewrite the above as

$$S_d = A\,S\;;\; A = I - cK_p^{-1}\,, \tag{22}$$

where I is the 3×3 identity matrix. Since both S_d and S are unit vectors, pre-multiplying (22) by S_d^t yields

$$1 = S_d^t S_d = S_d^t A S = S^t A^2 S\,. \tag{23}$$

Since (23) holds for all $\|S\| = 1$, we conclude that

$$A^2 = I\,,$$

hence A can be either I or $-I$. In other words, there are two equilibria, namely, $S = S_d$ and $S = -S_d$. In what follows, we will show that $S = -S_d$ is not a stable equilibrium.

Consider $S = -S_d$, and at steady state the Lyapunov function converges to $V_{ss}(\omega, S) = 2S_d^t K_p S_d$. Let S_ϵ to denote a small perturbation of S from $-S_d$, that is

$$S_\epsilon = -(1 - 2\epsilon)S_d\,,$$

where $\epsilon < 1$ is a small positive number. Then,

$$\begin{aligned}
V_\epsilon &= \tfrac{1}{2}(S_\epsilon - S_d)^t K_p(S_\epsilon - S_d) \\
&= (1 - \epsilon)^2 2\,S_d^t K_p S_d \\
&= (1 - \epsilon)^2 V_{ss} \\
&< V_{ss}
\end{aligned}$$

for $\epsilon > 0$. This implies that when S is perturbed from $-S_d$, V_ϵ will continue to decrease. Hence, $S = -S_d$ is an unstable equilibrium. In space operations, since spacecraft is exposed to a number of environmental disturbance torques, spacecraft attitude will eventually converge to $S = S_d$. Therefore, the function V given in (18) is indeed a Lyapunov function for Σ_c. This completes the proof.

It should be noted that the selection of (a_x, a_y, a_z) depends on the desired spacecraft performance for specific mission scenario. In the next, we present the adaptive control scheme for parameter $\bar{a}$.

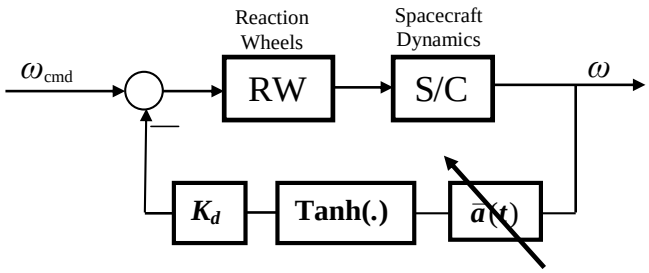

Figure 3. Inner velocity loop with adaptive parameters

IV. Adaptive Velocity Feedback Control

In practical two loop control design, the inner velocity feedback loop has wider bandwidth than the outer attitude/position loop, hence in comparison the velocity response is much faster. In particular, in the case of bounded controller proposed in (12), we can consider it running at two different time scales; slow and fast. The closed-loop stability has already been shown for both time scales, here we will focus on fast inner velocity loop and introduce an adaptive control scheme for improving performance; see Figure 3.

For inner velocity loop, we examine the spacecraft dynamics at a short time duration, hence the velocity Sigmoid term in (12) can be approximated by a linear function. Let $\bar{a} = (a_x, a_y, a_z)$ be a function of time t and given by

$$\bar{a}(t) = a_0 + \tilde{a}(t)\,, \tag{24}$$

where $a_0 = (a_1, a_2, a_3)$ and $a_i > 0$ are some arbitrarily small numbers and $\tilde{a}(t) = (\tilde{a}_x(t), \tilde{a}_y(t), \tilde{a}_z(t))$ are adaptive parameters. Considering only the velocity feedback and very short time duration, the closed-loop system resulted from closing only the inner loop becomes

$$J\dot{\omega}(\tau) = J\,\omega(\tau) \times \omega(\tau) - \tilde{K}_d(\tau)\omega(\tau)\,, \tag{25}$$

where τ is scaled from t indicating the 'fast' time scale and $\tilde{K}_d(\tau)$ is a diagonal matrix defined by

$$\tilde{K}_d(\tau) = \mathrm{diag}\left\{K_{dx}(a_1 + \tilde{a}_x(\tau)), K_{dy}(a_2 + \tilde{a}_y(\tau)), K_{dz}(a_3 + \tilde{a}_z(\tau))\right\}\,.$$

Consider the following candidate Lyapunov function for (25),

$$V = \frac{1}{2}\omega^t J\omega + \frac{1}{2}\tilde{a}_x^2\gamma_1^{-1} + \frac{1}{2}\tilde{a}_y^2\gamma_2^{-1} + \frac{1}{2}\tilde{a}_z^2\gamma_3^{-1}\,,$$

where γ_i are arbitrary positive numbers. Then, the time derivative of V along any solution of (25) is given by

$$\begin{aligned}
\dot{V} &= \omega^t(J\,\omega \times \omega) - \omega^t\tilde{K}_d\omega + \tilde{a}_x\dot{\tilde{a}}_x\gamma_1^{-1} + \tilde{a}_y\dot{\tilde{a}}_y\gamma_2^{-1} + \tilde{a}_z\dot{\tilde{a}}_z\gamma_3^{-1} \\
&= -\omega_x^2 a_1 K_{dx} - \omega_y^2 a_2 K_{dy} - \omega_z^2 a_3 K_{dz} + (\tilde{a}_x\dot{\tilde{a}}_x\gamma_1^{-1} - \omega_x^2 K_{dx}\tilde{a}_x) + (\tilde{a}_y\dot{\tilde{a}}_y\gamma_2^{-1} - \omega_y^2 K_{dy}\tilde{a}_y) \\
&\quad + (\tilde{a}_z\dot{\tilde{a}}_z\gamma_3^{-1} - \omega_z^2 K_{dz}\tilde{a}_z)
\end{aligned}$$

and if we choose the adaptive parameters as

$$\begin{aligned}
\dot{\tilde{a}}_x &= \gamma_1\omega_x^2 K_{dx}\,, \\
\dot{\tilde{a}}_y &= \gamma_2\omega_y^2 K_{dy}\,, \\
\dot{\tilde{a}}_z &= \gamma_3\omega_z^2 K_{dz}\,,
\end{aligned} \tag{26}$$

then we will have $V < 0$ for all $\omega \neq 0$, and hence V is a Lyapunov function for (25). Therefore, the adaptive scheme for parameters $(\tilde{a}_x, \tilde{a}_y, \tilde{a}_z)$ are given by (26).

V. An Illustrative Example

The proposed sun safe-hold bounded controllers developed in the previous section is applied to a small spacecraft. The control objective is to align the solar panels with the sun vector in order to maximize the power. The moments of inertia (kg-m^2) of the spacecraft are chosen to be: $I_{xx} = 50$, $I_{yy} = 70$, and $I_{zz} = 100$. The maximum reaction wheel torque is 30 mN-m, and there are four reaction wheels onboard the spacecraft and they are placed in a pyramid configuration with 45° base angle. The initial spacecraft body rates are assumed to be $\omega(0) = [0,\ 0,\ 0.01]$deg/sec, and the initial sun vector is chosen to be $S(0) = [0.7071,\ 0.7071,\ 0]$; a unit vector on the XY-plane. In this simulation, the target sun vector S_d is set to be a unit vector pointing along the Z-axis, i.e. $S_d = [0,\ 0,\ 1]$. The maximum control torque limits (with 50% margins) in body axis are: $(\bar{u}_x, \bar{u}_y, \bar{u}_z) = (0.022,\ 0.022,\ 0.044)$N-m.

Figures 4 and 5 show the simulation results with adaptive slope function $\bar{a}(t)$, and Figures 6 to 7 the time history of adaptive parameters $(\tilde{a}_x, \tilde{a}_y, \tilde{a}_z)$. As can be seen that the adaptive parameters reach the steady state values, and these values seem to be appropriate for the inner velocity loop response.

VI. Summary

This paper presents the sun safe-hold control system design by taking into account of the limited control torque. A PD-type bounded nonlinear controller is proposed by utilizing matrix gains, instead of scalar gains. The global asymptotic stability for feedback-controlled system is proved by applying Lyapunov's 2nd method. By applying the time scale seperation between the sun vector attitude loop and velocity loop, an adaptive control scheme is proposed and the simulation results show the effectiveness of the design.

References

[1]Markley, F. Landis, and John D. Nelson, "Zero-Gyro Safemode Controller for the Hubble Space Telescope." *Journal of Guidance, Control, and Dynamics*, Vol. 17, No. 4, 1994, pp. 815-822.

[2]Bourkland, Kristin L., Scott R. Starin, and David J. Mangus, "The Use of a Gyroless Wheel-Tach Controller in SDO Safehold Mode" *Flight Mechanics Symposium*, 2005.

[3]Starin, Scott R., and Kristin L. Bourkland, "Persistent Attitude Error in a Sun-Pointing Controller due to Nonlinear Dynamics," *AIAA Guidance, Navigation and Control Conference*, Hilton Head, SC, 2007.

[4]http://science.nasa.gov/missions/grail/

[5]Wen, John T.Y. and K. Kreutz-Delgado, "'The Attitude Control Problem," *IEEE Trans. on Automatic Control*, Vol. 36, No. 10, 1991, pp. 1148-1162.

[6]Wie, B., H. Weiss, and A. Arapostathis, "'Quaternion Feedback Regulator for Spacecraft Eigenaxis Rotations," *Journal of Guidance*, Vol. 12, No. 3, 1989, pp. 375-380.

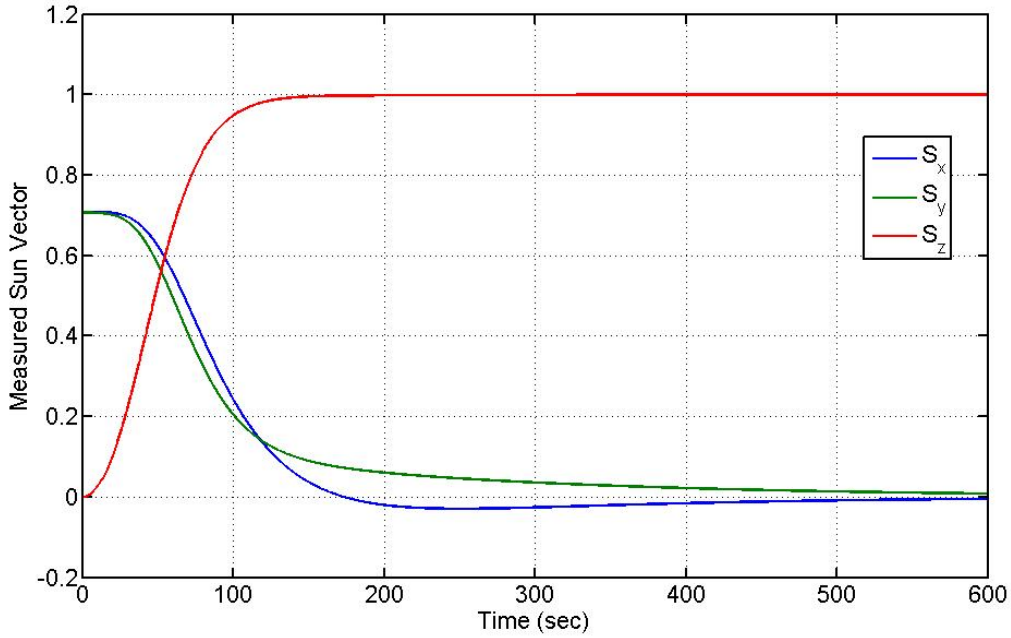

Figure 4. Measured sun vector relative to spacecraft body axis

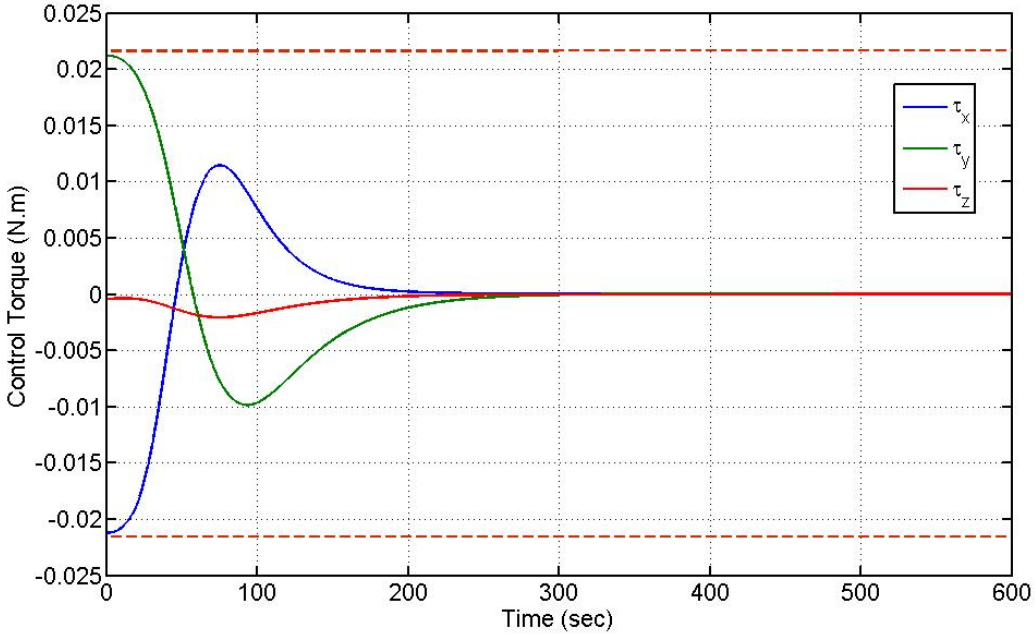

Figure 5. Control torques in body axis

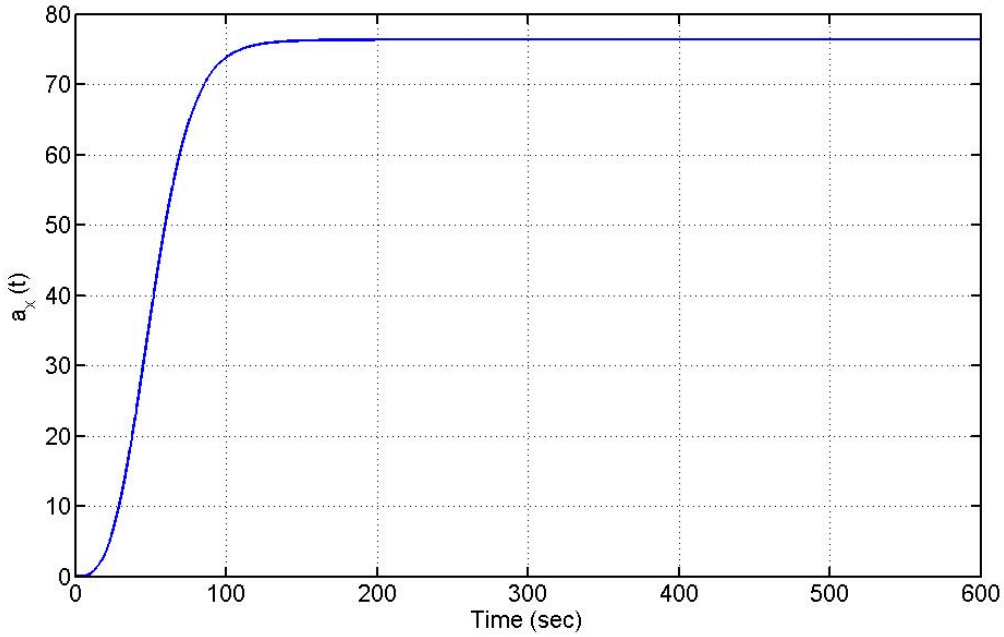

Figure 6. Adaptive parameter $\tilde{a}_x$

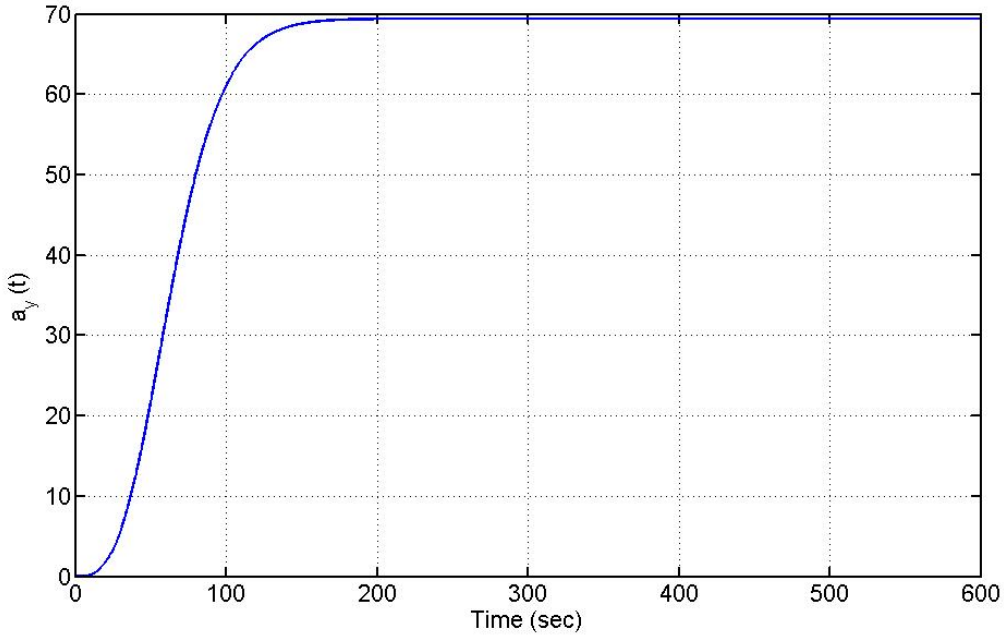

Figure 7. Adaptive parameter $\tilde{a}_y$

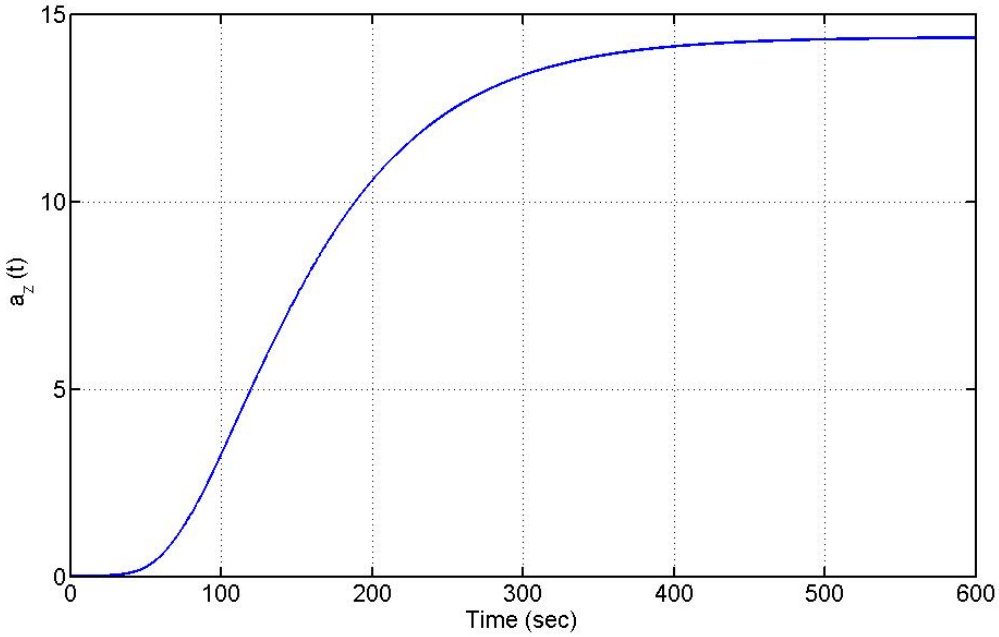

Figure 8. Adaptive parameter $\tilde{a}_z$